Machine Learning-Based Snow Cover Mapping in Uttarkashi, Chamoli and Pithoragarh Using Cloud Based Remote Sensing Tool

Shikha Goswami† and Alaknanda Ashok

College of Technology, G.B. Pant University of Agriculture and Technology, Pantnagar, Uttarakhand, India

†Corresponding author: Shikha Goswami; shikhagoswami.it@gbpuat-tech.ac.in

ORCID IDs of Authors https://orcid.org/0000-0002-7684-2517

Key Words	Classification and regression tree, Random forest, Support vector machine, Sentinel-2, Snow cover, Machine learning, Earth engine, Remote sensing, Confusion matrix, Land use land cover
DOI	https://doi.org/10.46488/NEPT.2026.v25i02.B4354 (DOI will be active only after the final publication of the paper)
Citation for the Paper	Goswami, S. and Alaknanda Ashok, 2026. Machine learning-based snow cover mapping in Uttarkashi, Chamoli and Pithoragarh using cloud based remote sensing tool. *Nature Environment and Pollution Technology*, 25(2), B4354. https://doi.org/10.46488/NEPT.2026.v25i02.B4354

ABSTRACT

Snow cover monitoring is essential for hydrological modelling, climate change analysis, and water resource management, especially in the Himalayan cryosphere. The most cutting-edge global open-source platform for sophisticated geospatial big data analysis is Google Earth Engine (GEE). This study leverages Google Earth Engine (GEE) and data sets available, that is Harmonized Sentinel-2 imagery, VIIRS, and Digital Elevation to delineate annual snow cover in Uttarkashi, Chamoli, and Pithoragarh districts of Uttarakhand. This paper aims to (i) Land Use Land Cover (LULC) Mapping. (ii) Detection of Snow cover in the Himalayan region districts of Uttarkashi, Chamoli, and Pithoragarh, Uttarakhand, India, using the annual composite median of Sentinel-2 imagery. (iii) To compare the performance of various machine learning models, that is Random Forest (RF), Support Vector Machine (SVM), and Classification and Regression Tree (CART) for 5 classes. (iv) To calculate the area of 5 classes for the years 2019 and 2024. (v) To build classified maps using the algorithm that results in the best overall accuracy. Here, three machine Learning approaches Random Forest (RF), Support Vector Machine (SVM), and Classification and Regression Tree (CART) are trained using input parameters such as bands, spectral indices (NDVI, NDBI, NDSI, BSI), and topographic parameters (elevation, slope) derived from ALOS DEM. Cloud-masking techniques refine the dataset, ensuring high-quality spectral inputs. The result demonstrated the successful mapping of LULC's five land cover classes: bare soil, snow, vegetation, built-up areas, and water bodies. The study demonstrated high classification accuracy in 2019 for RF, SVM, and CART across all districts, achieving 95.7%, 93.2%, and 90.7% in Chamoli; 96.5%, 97.3%, and 95.6% in Pithoragarh; and 88.6%, 90.0%, and 87.3% in Uttarkashi. In 2024, the accuracy rates improved to 96.2%, 93.9%, and 94.6% for Chamoli; 95.8%, 92.5%, and 91.6% for Pithoragarh; and showed significant gains reaching 95.4%, 95.4%, and 96.1% for Uttarkashi. Results indicated that estimated In Chamoli, RF consistently performed better, demonstrating an 8.3% increase in snow from 2,206 km² to 2,388 km², while Pithoragarh experienced a 25% loss from SVM to RF: from 2,099 km² to 1,573 km²).Snowfall in Uttarkashi increased by 10.8% from SVM to CART: from 1,804 km² to 1,998 km2, with

CART doing exceptionally well in 2024.RF proved most reliable overall, but regional variability suggests need for adaptive model selection.

1. INTRODUCTION

The mapping of Land Use Land Cover (LULC) using a variety of remotely sensed datasets, such as optical, Synthetic Aperture Radar (SAR), Unmanned Aerial Vehicle (UAV), and others, is the primary application of remote sensing technologies (Lu and Weng, 2007; Goswami Shikha; Ashok Alaknanda, 2024). Numerous practical uses, such as flood mapping, disaster management, future disaster preparedness, rehabilitation and reconstruction prioritization, effective land-use planning, and natural resource management, benefit from the classification and identification of different land cover types (S, 2018; Tsai *et al.*, 2019; KHANDURİ, 2021; Rawat *et al.*, 2022; Siddique, Haris and Pradhan, 2022; Saini and Rawat, 2023). Unlike a conventional plain area, the Himalayan region has a unique geography, with many rivers, glaciers, and high mountain ranges (S, 2018). Understanding a range of natural and human systems requires constant monitoring of the quantity of snow cover, which can be accomplished practically via remote sensing.

The higher Himalayan region is susceptible to several natural hazards because of factors like freeze-thaw cycles, thrusts and faults, earthquakes, high relief, few valleys, steep slopes, intense rainfall, and temperature fluctuations. Finding places that are more vulnerable to these types of natural disasters and creating mitigation plans can both be facilitated by an understanding of the region's LULC trends. Also, classifying land use and land cover, or LULC, is essential for controlling resource depletion in emerging areas and lessening the effects of population increase. Effective LULC classification aids in mitigating the negative effects of urbanization's rapid expansion on global energy resources, facilitating resource management, sustainable planning, and environmental preservation (Avtar *et al.*, 2019). According to (Qu and Long, 2018; Stehfest *et al.*, 2019), accurate LULC maps of a region can assist in classifying the land into major classes to provide an overview of the resources, their use, and their influence on the socioeconomic development of the area. Additionally, it can assist researchers in examining a range of environmental challenges at different sizes. Another important indicator of climate change is the alteration in LULC (Li *et al.*, 2022). Furthermore, the water balance of that specific area is always disrupted by changes in the climate (Sridhar, Jin and Jaksa, 2013; Sridhar, Kang and Ali, 2019)geomorphology and LULC patterns(Duda and Hart, 1974). A thorough LULC map is therefore necessary as a dynamic element for the monitoring of water quantity and quality(Tariq *et al.*, 2021, 2023) land management(Asif *et al.*, 2023; Zheng *et al.*, 2023) hazards, and risk assessment(Goswami Shikha; Ashok Alaknanda, 2024). In order to manage the land use in the area, high-resolution data processed using creative and sophisticated geospatial techniques (Dou *et al.*, 2021) are crucial. The region frequently experiences hazards like avalanches, rockfalls, debris flows, and cloudbursts, and as a result of altered weather patterns, their frequency and intensity have increased(Bhatt *et al.*, 2014). In addition to playing a major role in a nation's economic development, natural resources like forests are crucial for preserving a region's biodiversity, climate, ecological balance, and water conservation. One of the most important indicators of the general health of the biological system in the area is the state of the forests. Natural catastrophes can happen at any time and are growing more frequent (Siddique, Haris and Pradhan, 2022). Understanding climate, ecology, and water cycles requires regular monitoring of snow cover(Nijhawan, Das and Raman, 2019).

Abdi(Abdi, 2020) evaluated the performance of four different machine learning algorithms in classifying land cover using Sentinel-2 satellite data in a complex mixed-use area in south-central Sweden. Four methods were investigated in this study: deep learning, Extreme Gradient Boosting (Xgboost), Random Forests (RF), and Support Vector Machines (SVM). The study found that SVM, with an overall accuracy score of 75.80%, was closely followed by the Xgboost classifier. The study also discovered that Sentinel-2 bands in the red edge and shortwave infrared regions of the spectrum were crucial to the classification process. Using Sentinel-2 data(Saini and Ghosh, 2018b) also classified crops using RF and SVM classifiers. The results indicated that while SVM reported an overall accuracy of 81.85%, RF (84.22%) achieved the best classification accuracy. Additionally, their study demonstrated how beneficial Sentinel-2 data is for mapping vegetation. In a different study, the authors used supervised learning for LULC mapping and used hybrid, optical, and microwave datasets (Sentinel-2, Sentinel-1, respectively) (Chachondhia, Shakya and Kumar, 2021). Every dataset was assessed using the RF and SVM machine learning (ML) algorithms. In terms of classification outcomes, the optical and hybrid datasets performed better than the microwave dataset (Noi and Kappas, 2017) conducted another LULC investigation using Sentinel-2 satellite data, and they evaluated the effectiveness of k Nearest Neighbour (KNN), RF, and SVM classifiers. According to this comparative analysis, SVM (95.32%) achieved somewhat better accuracies for KNN (94.59%) and RF (94.70%). Using Sentinel-2 satellite images from 2022, machine learning algorithms such as CART (Oliveira *et al.,* 2012), SVM (Oliveira *et al.,* 2012), and random forest (RF) (Choubin *et al.,* 2019) can produce accurate and educational LULC maps. Key land cover features in the study area, such as vegetation, built-up areas, barren land, and water bodies, can be identified using a variety of satellite indices, including the Normalized Difference Vegetation Index (NDVI) (Defries and Townshend, 1994), Modified Normalized Difference Water Index and Normalized Difference Built Index (NDBI) (Shen *et al.,* 2019). With Kappa coefficients and overall accuracy metrics acting as important performance indicators, the effectiveness of the three machine learning models (CART, SVM, and RF) may be assessed through validation and accuracy evaluations. According to the study(Abdi, 2020), GEE can interpret Sentinel-2 satellite images effectively enough to generate LULC maps for the four land cover classes that are defined with accuracy and dependability. With an emphasis on model performance, feature recognition, accuracy evaluations, and the effectiveness of GEE in processing satellite images, this study tackles a number of issues pertaining to the application of machine learning techniques(Pushpalatha *et al.,* 2024) within Google Earth Engine for LULC mapping. The results demonstrate the ability of GEE and three machine learning models (CART, RF, and SVM) for generating trustworthy LULC maps, particularly when applied to land-use and environmental research. Improved accuracy and robustness are made possible by combining geospatial methods for LULC analysis with three machine learning models—RF, SVM, and CART(Chachondhia, Shakya and Kumar, 2021). We can obtain more accurate and thorough LULC classification results by combining the advantages of these models and utilizing geospatial data, which will capture the intricate spatial relationships and patterns inherent in land use dynamics. In a recent work, (Boonpook *et al.,* 2023) evaluated the ability of a deep learning model named LoopNet to autonomously categorize land use using Landsat-8 images(Nijhawan, Das and Balasubramanian, 2018). The results show that LoopNet performed better than SVM and RF (overall accuracy = 89.84%). Sentinel satellites, both optical and radar, were used by (Billah *et al.,* 2023) to track floods and evaluate damage in northeastern Bangladesh. With a 90% accuracy rate for mapping land cover, the RF classifier was shown to be more efficient than other Machine Learning Classifiers. Sentinel-2 data and the RF method were utilized to analyse LULC change in Vietnam. For time series datasets, the approach produced high accuracy (for both the 2019 (90.7%) and 2020

(91.1%) datasets). India is especially susceptible to natural disasters due to its diversified geology, climate, geomorphology, vegetation, geography, and sizable population. The Himalayan region's seismic-tectonic instability makes it particularly vulnerable to different mass wasting events. While prompt planning and action can greatly lessen the effects of natural disasters and return things to normal, they can also be prevented to a large degree. In order to address each disaster planning issue, a thorough evaluation of LULC in the area may be quite helpful. By applying three machine learning techniques, RF, SVM, and CART, for classification in the Chamoli, Pithoragarh and Uttarkashi districts of Uttarakhand, India, this work aims to create useful snow cover maps and land use land cover(Saini and Singh, 2024). The viability of employing satellite Sentinel-2 imagery for this purpose will also be examined.

2. DATA AND STUDY AREA

The study utilizes the following datasets:

- **Sentinel-2 Surface Reflectance (S2_SR_HARMONIZED)**(Claverie *et al.,* 2018)**:** Optical imagery for vegetation, water, and built-up land classification.
- **ALOS AW3D30 DEM** (Tadono *et al.,* 2014): Elevation and slope data for terrain analysis.
- **VIIRS Stray Light Corrected Nighttime Day/Night Band**(Mills, Weiss and Liang, 2013)**:** enhances low-light imagery accuracy by removing stray light interference, enabling precise detection of nighttime emissions (e.g., urban lights, wildfires, auroras).
- **JRC/GSW1_4/Global Surface Water**(Pekel *et al.,* 2016)**:** The dataset helps distinguish between water bodies and snow/urban regions by mapping global water dynamics (1984–2021). Its incorporation with Sentinel-2 and DEM data may improve the precision of glacier lake, flood, and snowmelt monitoring.

The Northern Indian state of Uttarakhand is home to several breathtaking sights. However, it is particularly susceptible to a variety of natural disasters because of its unique climate, ecology, tectonic activity, and socioeconomic landscape. Earthquakes, landslides, avalanches, hailstorms, cloudbursts, flash floods, forest fires, and lightning strikes are among the many natural disasters that occur in the area. The establishment of hydroelectric power plants, riverbed mining, and the building of local roads and structures have all significantly altered the landscape, land use, and natural eco-geological systems. The study focuses on a specific region defined using the geometry variable in GEE. The northern Indian Himalayan state of Uttarakhand covers a variety of latitudes (28°43′ N to 31°27′ N) and lengths (77°34′ E to 81°02′ E). Its varied geography includes snow-covered Tibetan borders and the fertile Terai plains. Three districts Uttarkashi, Chamoli, and Pithoragarh, are at its centre, they are distinguished by their distinct geographic locations, cultural diversity, and ecological importance.

The study examines the snow cover in three Uttarakhand Himalayan districts: Uttarkashi, Chamoli, and Pithoragarh. These districts are vital to the state's ecology, with the Ganges fed by glaciers in Uttarkashi, Chamoli blending biodiversity and spirituality, and Pithoragarh bordering Nepal and Tibet. The study reveals five critical LULC classes in these districts: built-up, snow, vegetation, water, and bare lands, highlighting the need for close monitoring of their delicate ecosystems. The research regions in Uttarakhand, India, are depicted in the Figure 1 along with their elevation. A map of India is displayed in image (a), with the state of Uttarakhand highlighted to

denote the study area. Detailed elevation maps of the districts of Uttarkashi, Chamoli, and Pithoragarh are shown in images (b), (c), and (d), respectively.

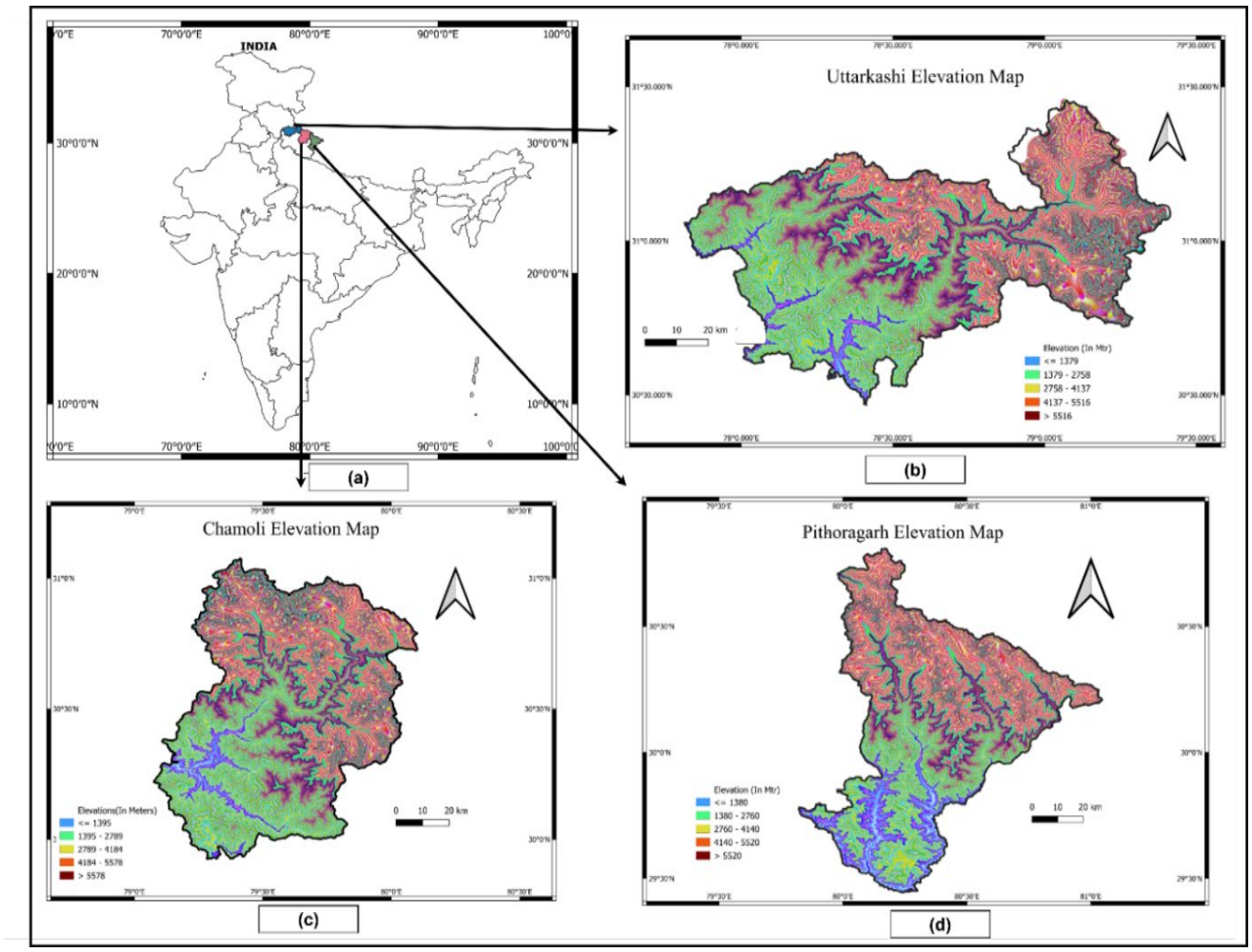

Figure 1: Location of study area, a Map of India, i.e, location of study area in Uttarakhand state, b Uttarkashi District, c. Chamoli District, d. Pithoragarh District

Elevation ranges are represented on these maps using color-coded gradients, where red/brown denotes higher altitudes and blue denote lower elevations. ≤1379 m (blue), 1379–2758 m (green), 2758–4137 m, (yellow), 4137–5516 m (red), and >5516 m (brown) are the height zones of Uttarkashi. With comparable colour schemes, Chamoli and Pithoragarh range from ≤1395 m to >5578 m and ≤1380 m to >5520 m, respectively. Understanding topography and hydrological patterns are aided by the display of rivers and contour variations.

3. METHODOLOGY

The proposed methodology for Land Use Land Cover(Kadavi and Lee, 2018) Classification Snow cover mapping is depicted in the proposed method begins with an annual Harmonized Sentinel-2 MSI, VIIRS Stray light corrected Nighttime Day/Night Band, Digital Elevation Model (ALOS DSM: Global 30m v3.2) and WWF HydroSHEDS satellite imageries acquisition process for the years 2019 and 2024, followed by data preparation. We employed Google Earth Engine's pre-processed Sentinel-2 Surface Reflectance (SR) dataset, which includes applied atmospheric and radiometric corrections, eliminating the need for additional processing. For our comparative analysis between 2019 and 2024, we acquired all available scenes with less than 20% cloud cover from two annual periods: January-December 2019 and January-December 2024. All selected images were at the native 10-meter

spatial resolution. Using modal compositing to minimize cloud and aerosol effects, we generated multispectral image tiles for each year by stacking the Blue (B2: 490 nm), Green (B3: 560 nm), and Red (B4: 665 nm) spectral bands.The study area boundary was delineated using a shapefile obtained from the Survey of India (https://www.surveyofindia.gov.in/). Training data points were generated through a combination of spectral indices derived from Harmonized Sentinel-2 MSI, VIIRS Stray light corrected Nighttime Day/Night Band, Digital Elevation Model (ALOS DSM: Global 30m v3.2) and WWF HydroSHEDS datasets, visual interpretation of Sentinel-2 imagery, and validation using high-resolution Google Earth basemaps. When machine learning classifiers are trained on the dataset, the data analysis process starts. Two parts of the reference dataset are separated, one for testing and one for training, with a 70%:30% split, respectively. After that, the testing dataset is used to evaluate the classifiers' performance.

For classification utilizing remotely sensed data, machine learning methods such as RF, SVM(Kadavi and Lee, 2018), and CART are frequently employed (Qu and Long, 2018; Saini and Ghosh, 2018b, 2018a; Nijhawan, Das and Raman, 2019; Chachondhia, Shakya and Kumar, 2021; Dou et al., 2021; Tariq et al., 2021; Billah et al., 2023). This study utilized three supervised machine learning approaches: RF, SVM, and CART, with ensemble learning involving decision trees to obtain useful LULC maps and snow cover.(Breiman, 2001). It can tolerate noisy, correlated characteristics and does well with multidimensional data. The remote sensing community regularly uses this classifier because it can successfully and efficiently handle a wide range of issues. Support Vector Machine (SVM) is a potent method designed especially to tackle regression and non-linear classification problems(Cortes and Vapnik, 1995). SVM divides high-dimensional feature spaces using hyperplanes, handling intricate datasets with high accuracy. However, careful selection of regularization parameters and kernel functions can be computationally costly. Classification and Regression Tree (CART) is a non-parametric, tree-based classifier that uses feature thresholds to partition data, minimizing impurity and generating interpretable decision rules for classification or regression tasks.(Breiman *et al.*, 2017) The CART algorithm, a rule-based classification and regression tool, can handle classification and regression tasks but is susceptible to overfitting, instability, and difficulty in identifying complex relationships in non-linear or unbalanced datasets. After training machine learning models, five LULC classes, i.e., Bare, Snow, Vegetation, Built-up, Water, are predicted using the testing dataset. For the evaluation process, a confusion matrix is produced by each classifier using the testing dataset.

3.1 Technical Workflow of the Proposed Methodology

Figure 2 explains the technical workflow of proposed methology which tells about the data sources, Pre-processing,methodology, feature extraction,traning and validation, classification algorithm,accuracy assessment and model comparison.

3.1.1. Data Sources:

- **Google Earth Engine**: The platform used for processing and analysing geospatial data.
- **VIIRS Stray Light Corrected Nighttime Day/Night Band**: Provides nighttime light data, useful for urban and human activity analysis.
- **Digital Elevation Model (ALOS DSM: Global 30m v3.2)**: Provides topographic data.
- **WWF HydroSHEDS**: Offers hydrological data like river networks and watersheds.

- **Study Area Shapefile**: Defines the geographic boundary for analysis, downloaded from the Survey of India.
- **MOD10A1.061 Terra Snow Cover Daily Global 500m:** Snow Cover Daily Global 500m product contains snow cover, snow albedo, fractional snow cover, and quality assessment (QA) data

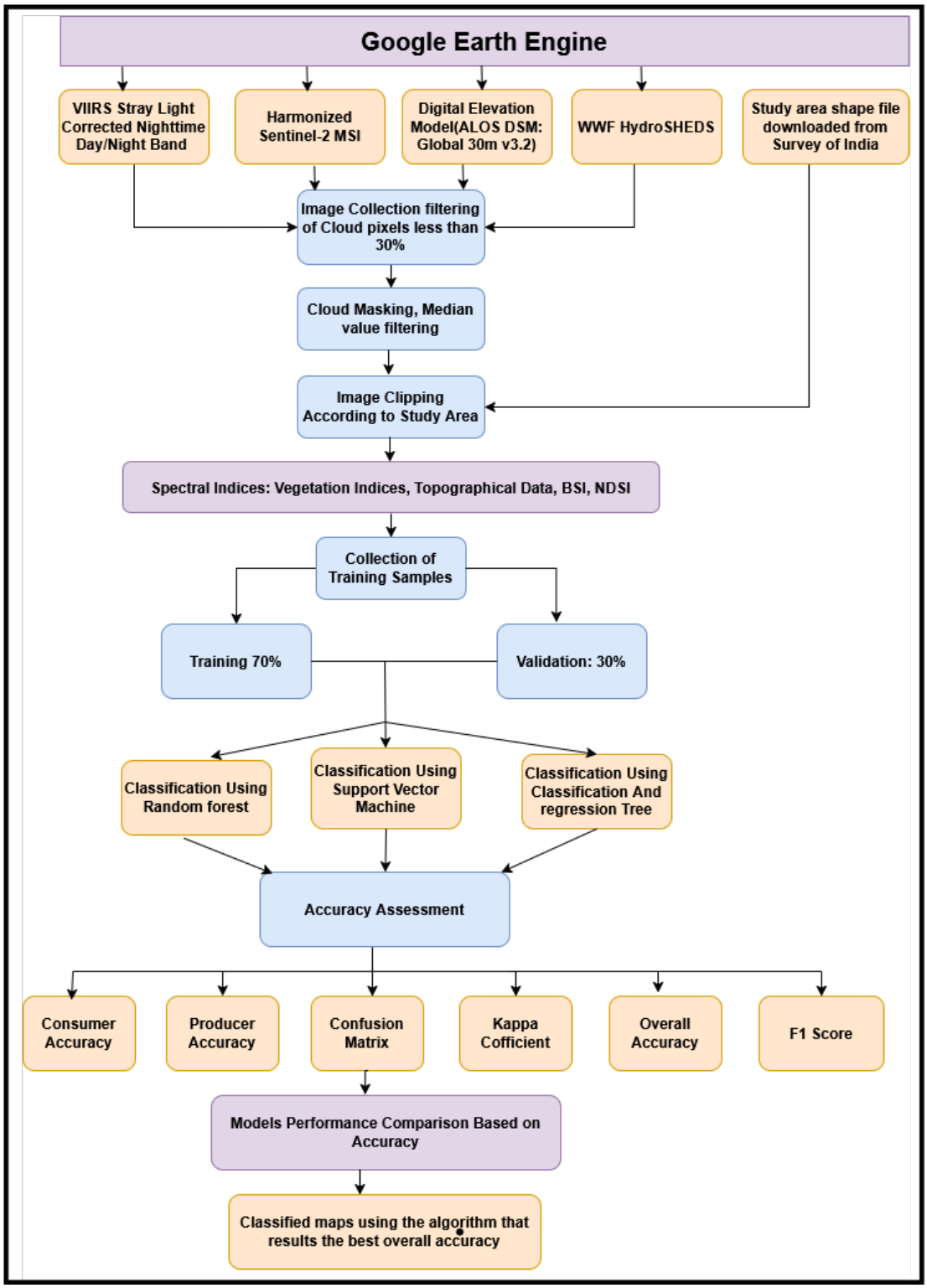

Figure 2: Workflow of the proposed methodology

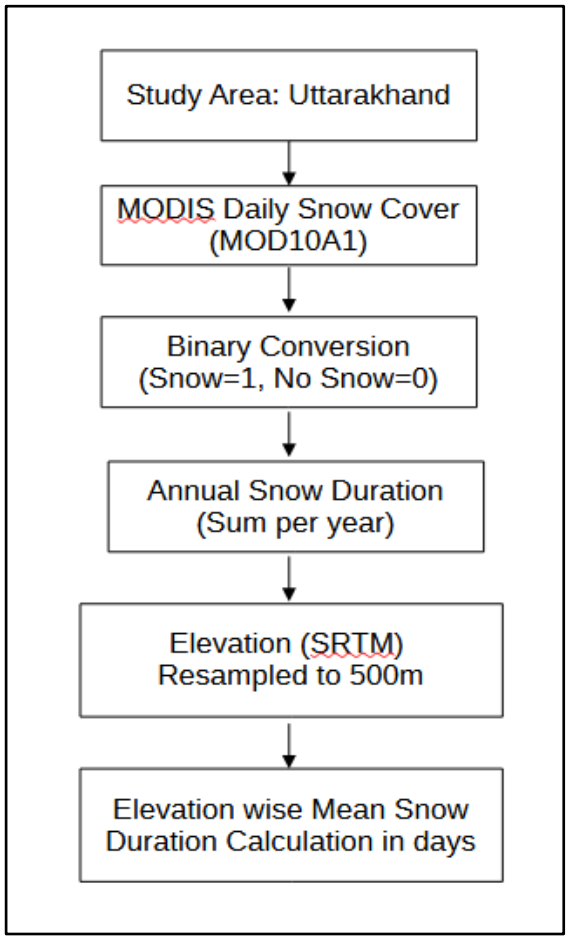

Figure 3 Workflow to calculate Snow Cover Duration Analysis for period of year (2000–2023)

3.1.2.Preprocessing:

- **Image Collection Filtering**: Filters out images with more than 30% cloud cover to ensure data quality.
- **Cloud Masking**: Removes cloud-contaminated pixels from the images.
- **Median Value Filtering**: Reduces noise by using median pixel values over a time series(Goswami and Ashok, 2024).
- **Image Clipping**: Crops the images to the study area boundary.

3.1.3. Feature Extraction:

- **Spectral Indices**: Calculates indices like Vegetation Indices (e.g., NDVI), Bare Soil Index (BSI), Normalized Difference Snow Index (NDSI), and incorporates topographic data for enhanced classification. Table 1 Shows the formulas of varies indices.

3.1.4. Training and Validation:

- **Collection of Training Samples**: Gathers labelled data for supervised classification.
- **Data Splitting**: Divides the data into 70% for training and 30% for validation.

3.1.5. Classification Algorithms:

- **Random Forest**: An ensemble learning method for classification.
- **Support Vector Machine (SVM):** A kernel-based method for classification.
- **Classification and Regression Tree (CART):** A decision tree-based approach.

3.1.6. Accuracy Assessment:

- **Precision**: Measures how often the classifier correctly predicts a class.
- **Recall**: Measures how well the classifier represents relevant positive cases out of all actual positives.
- **Confusion Matrix**: A table showing true vs. predicted classifications.
- **Kappa Coefficient**: Evaluates classifier agreement beyond chance.
- **Overall Accuracy**: The total percentage of correctly classified pixels.
- **F1 Score**: Balances precision and recall for class-specific accuracy.

3.1.7. Model Comparison and Output:

- **Models Performance Comparison**: Compares the accuracy of Random Forest, SVM, and CART to select the best-performing algorithm.
- **Classified Maps**: The final output is a land cover map generated using the algorithm with the highest overall accuracy.

Table 1: Spectral Indices Formulas

Index	Formula	Purpose
NDVI	(B8-B4)/(B8+B4)	Vegetation Health
NDBI	(B11-B8)/(B11+B8)	Built-up Areas
MNDWI	(B3-B11)/(B3+B11)	Water Bodies
BSI	((B6+B4) -(B2+B11))/((B6+B4) +(B2+B11))	Bare Soil Detection
NDSI	(B3-B11)/(B3+B11)	Snow

For each ML classifier (RF, SVM, and CART), a variety of evaluation parameters are generated from the confusion matrix, including overall accuracy, precision, recall, F-score, and kappa coefficient. The following is a definition of the utilized parameters:

(i) **TP**: True Positive, which stands for the total number of samples that were correctly classified.

(ii) **TN**: the sum of all samples for which the negative class is properly predicted by the model.

(iii) **FP**: False Positive, which stands for the total number of incorrectly classified samples that belong to several classes but were wrongly assigned to a specific class.

(iv) **FN**: False Negative is classification error occurs when a sample of a given class is mistakenly categorized as not belonging to that class.

Another often-used parameter for remote sensing classification applications is the Kappa Coefficient, which ranges from 0 to 1. It illustrates the discrepancy between the actual and improbable(expected) agreements. A Kappa score of 0 indicates that there is no agreement between the reference image and the classified image. On the other hand, a kappa value of 1 indicates that the reference image and the classified image are identical. Therefore, the more precise the classification, the greater the kappa value (ka). Equations 1, 2, 3, 4, and 5 are used, successively, to produce a variety of metrics, including accuracy, precision, recall, F1-score, and kappa values.

$$\textbf{\textit{Accuracy}} = \frac{\textit{True Positive} + \textit{True Negative}}{\textit{True Positive} + \textit{True Negative} + \textit{False Negative} + \textit{False Positive}} \quad (1)$$

$$\textbf{\textit{Precision}} = \frac{\textit{True Positive}}{\textit{True Positive} + \textit{False Positive}} \quad (2)$$

$$\textbf{\textit{Recall}} = \frac{\textit{True Positive}}{\textit{True Positive} + \textit{False Negative}} \quad (3)$$

$$\textbf{\textit{F1 – Score}} = 2 * \frac{\textit{Precision} * \textit{Recall}}{\textit{Precision} + \textit{Recall}} \quad (4)$$

$$\textbf{\textit{kappa}} = \frac{\textit{observed accuracy} - \textit{chance agreement}}{1 - \textit{chance agreement}} \quad (5)$$

RESULT AND DISCUSSION

The VIIRS Stray Light Corrected Nighttime Day/Night Band, Harmonized Sentinel-2 MSI, Digital Elevation Model (ALOS DSM: Global 30m v3.2), WWF HydroSHEDS satellite datasets are used in this study to classify LULC and map snow cover in the Himalaya region using RF, SVM, and CART classifiers. One of the most biologically varied areas of the globe, the Himalayas are home to a variety of habitats, including subtropical forests, alpine meadows, and glaciers. The area's forests and snow are vital parts of its ecology, offering a number of significant advantages that are vital to the environment and its inhabitants. Some of the world's biggest and most significant rivers, such as the Ganges, Brahmaputra, and Indus, are found in the Himalayan region. The snow and ice that build up on the area's mountains and glaciers feed these rivers. The rivers wouldn't have enough water to support the local ecosystems and population without this snow and ice. Thus, snow cover mapping and LULC classification are essential data for decision-making and the research area's sustainable development. The reference dataset was gathered using Google Earth Engine and Training data points were generated through a combination of spectral indices derived from the Harmonized Sentinel-2 MSI, VIIRS Stray light corrected Nighttime Day/Night Band, Digital Elevation Model (ALOS DSM: Global 30m v3.2) and WWF HydroSHEDS datasets, visual interpretation of Sentinel-2 imagery, and validation using high-resolution Google Earth basemaps. It was then split into 70:30 ratios, with 30% of the samples being used for testing and 70% of the reference samples being utilized for training. Each land cover class has its own exclusive partitioning of the reference data pixels. to put into practice the RF, SVM, and CART machine learning techniques. Higher statistical accuracy in remote sensing is a sign of more precise maps of snow cover and LULC. In this study, the F1-score, Precision, and Recall were employed to determine class-specific accuracy, while the confusion matrix was used to compute the overall accuracy and the kappa coefficient. The effectiveness of the RF, SVM, and CART algorithms for classification was assessed using a suitable sampling dataset. Estimates of the producer's (recall) and user's (precision) accuracy for each spatial cover class, as well as the F1-score, overall accuracy, and kappa coefficient as a general measure of the classification finding’s efficacy, were calculated using the confusion matrices of these algorithms.

Table 2: Classifier overall accuracy and kappa coefficient obtained by RF, SVM, CART

Region	Model	2019		2024	
	ML Classifiers	OA (%)	Kappa (%)	OA (%)	Kappa (%)
Chamoli	RF	95.7	95.7	96.2	96.2
	SVM	93.2	91.3	93.9	91.8
	CART	90.7	88.1	94.6	92.8
Pithoragarh	RF	96.5	95.5	95.8	94.5
	SVM	97.3	96.6	92.5	90.1
	CART	95.6	94.3	91.6	89.2
Uttarkashi	RF	88.6	85.6	95.4	94.2
	SVM	90	87.3	95.4	94.2
	CART	87.3	84	96.1	95.1

This study of comparative analysis evaluates three machine learning classifiers RF, SVM, and CART for land use/land cover classification across three Himalayan regions (Chamoli, Pithoragarh, and Uttarkashi) between 2019 and 2024 shown in Table 2. The results demonstrate RF's superior consistency, maintaining high accuracy (OA >95.7%) and reliability (Kappa >94.5%) across all regions with minimal fluctuations (±0.7%). While SVM and CART showed remarkable improvements in Uttarkashi (CART: +8.8% OA, +11.1% Kappa; SVM: +5.4% OA, +6.9% Kappa), they exhibited significant declines in Pithoragarh (SVM: -4.8% OA, -6.5% Kappa; CART: -4.0% OA, -5.1% Kappa). Chamoli witnessed steady performance across all models, with CART showing the most

improvement (+3.9% OA, +4.7% Kappa). The strong OA-Kappa correlation (differences <2%) confirms classification reliability, though SVM and CART's regional performance variations highlight their sensitivity to local conditions, contrasting with RF's robust generalization across diverse terrains and temporal changes. These findings suggest RF's suitability for regional-scale LULC mapping, while SVM and CART may require location-specific tuning for optimal performance For LULC classification, this work assesses RF, SVM, and CART classifiers in three Himalayan regions (2019–2024). The acronyms used before delving deeper into confusion matrix and calculated accuracy measures for particular LULC class are described Table 3. RF proved to be the most dependable because to its remarkable stability (OA>95.7%, Kappa>94.5%) and low variations (±0.7%). Both SVM and CART had a dramatic reduction in Pithoragarh (SVM: -4.8% OA; CART: -4.0% OA), whereas they shown notable improvements in Uttarkashi (CART: +8.8% OA; SVM: +5.4% OA). Across models, Chamoli's performance remained consistent, with CART seeing noteworthy increases (+3.9% OA). The veracity of the results is confirmed by the significant OA-Kappa correlation (less than 2% difference). The results highlight the significance of context-aware model selection in LULC mapping by recommending RF for reliable regional applications and requiring location-specific tuning for SVM/CART because of their sensitivity to local variables.

Table 3: Abbreviations for various land use Land cover

Abbreviation	Full Form	Description
RF	Random Forest	A machine learning classifier based on ensemble decision trees.
SVM	Support Vector Machine	A supervised learning model used for classification/regression.
CART	Classification and Regression Tree	A decision tree-based algorithm for classification or regression tasks.
OA	Overall Accuracy	Overall classification accuracy across all classes.
SC	Snow Cover	Land cover class representing snow-covered areas.
VC	Vegetation Cover	Land cover class representing vegetated areas (e.g., forests, crops).
BU	Built-up	Land cover class representing urban or constructed areas.
Kappa	Kappa Coefficient	Statistical measure of inter-rater agreement, adjusted for chance.
F1	F1-score	The F1 score is the harmonic mean of precision and recall, balancing both to assess classification model performance.
LULC	Land Use Land Cover	Land Use Land Cover shows land's use and surface type.
NDVI	Normalized Difference Vegetation Index	NDVI (Normalized Difference Vegetation Index) measures vegetation health using satellite reflectance of red and near-infrared light.

This study provides the confusion matrices of the best classification outputs from RF, SVM, and CART, highlighting class-wise performance and patterns of misclassification in land use/land cover mapping.

Table 4: Normalised Confusion Matrix Chamoli produced by RF in 2019

		Classification (Predicted)					
	Actual \ Predicted	**Bare**	**Snow**	**Vegetation**	**Built-up**	**Water**	**Producer's Accuracy/Recall**
Ground Truth (Actual)	**Bare**	0.96	0	0	0.04	0	0.96
	Snow	0.04	0.96	0	0	0	0.96
	Vegetation	0	0	0.95	0	0	1
	Built-up	0.05	0.05	0	0.9	0	0.9
	Water	0	0	0	0.08	0.92	0.92
	Consumer's Accuracy/Precision	0.92	0.95	1	0.9	1	**Overall Accuracy = 95.7 %**

This multi-class classifier RF for Chamoli for year 2019 shown in Table 4 achieves 95.7% overall accuracy, with Vegetation (100% recall/precision) and Water (100% precision, 92% recall) performing best. Bare (96% recall, 92% precision) and Snow (96% recall, 4% Bare misclassification) show strong results, while Built-up (90% recall/precision) struggles with Bare/Snow overlap. NDWI/NDBI could improve Water-Built-up and spectral confusion. The model is reliable but refinable.

Table 5: Normalised Confusion Matrix Chamoli produced by RF in 2024

		Classification (Predicted)					
	Actual \ Predicted	**Bare**	**Snow**	**Vegetation**	**Built-up**	**Water**	**Producer's Accuracy/Recall**
Ground Truth (Actual)	**Bare**	0.97	0	0	0.03	0	0.97
	Snow	0	1	0	0	0	1
	Vegetation	0.03	0	0.97	0	0	0.97
	Built-up	0.18	0	0	0.82	0	0.82
	Water	0	0	0	0.14	0.86	0.86
	Consumer's Accuracy/precision	0.93	1	1	0.82	1	**Overall Accuracy = 96.2%**

The Chamoli 2024 classifier RF Shown in Table 5 achieves 96.2% accuracy, excelling in Snow (100% recall/precision) and Vegetation (97% recall, 100% precision)**.** Bare (97% recall, 93% precision**)** shows minor confusion with Built-up, which struggles (82% recall/precision, 18% misclassified as Bare). Water (100% precision, 86% recall) faces murky-water misclassification. Key challenges include Built-up ↔ Bare (urban expansion) and Water ↔ Built-up (spectral overlap). Improvements like GLCM texture analysis and NDBI/NDWI indices can enhance classification, though urbanization and climate change require adaptive refinements for Himalayan monitoring.

Table 6: Normalised Confusion Matrix Pithoragarh produced by SVM in 2019

		Classification (Predicted)					
	Actual \ Predicted	**Bare**	**Snow**	**Vegetation**	**Built-up**	**Water**	**Producer's Accuracy/Recall**
Ground Truth (Actual)	**Bare**	0.94	0	0.06	0	0	0.94
	Snow	0	1	0	0	0	1
	Vegetation	0.03	0	0.97	0	0	0.97
	Built-up	0	0	0	1	0	1
	Water	0.06	0	0	0	0.94	0.94
	Consumer's Accuracy/precision	0.88	1	0.97	1	1	**Overall Accuracy = 97.3 %**

The Pithoragarh 2019 SVM classifier shown in Table 6 achieves 97.3% accuracy, with Snow and Built-up (100% recall/precision) performing flawlessly. Vegetation (97% recall/precision, 3% Bare misclassification) and Water (100% precision, 94% recall, 6% Bare confusion) show strong results, while Bare (94% recall, 88% precision) faces minor misclassifications. Key challenges include spectral overlap in mixed pixels (Bare/Vegetation/Water)**.** Suggested improvements: textural features, NDVI (Vegetation), and NDWI (Water) for sharper class boundaries. Though reliable for Himalayan monitoring, the model needs refinement for urban planning and hydrology applications in complex terrain.

Table 7: Normalised Confusion Matrix Pithoragarh produced by RF in 2024

		Classification (Predicted)					
	Actual \ Predicted	**Bare**	**Snow**	**Vegetation**	**Built-up**	**Water**	**Producer's Accuracy/Recall**
Ground Truth (Actual)	**Bare**	0.97	0	0	0	0.03	0.97
	Snow	0.03	0.97	0	0	0	0.97
	Vegetation	0	0	0.96	0	0	1
	Built-up	0	0	0.12	0.88	0	0.88
	Water	0	0	0	0.11	0.89	0.89
	Consumer's Accuracy/precision	0.97	1	0.93	0.93	0.89	**Overall Accuracy = 95.8 %**

The Pithoragarh 2024 Random Forest classifier shown in Table 7 achieves 95.8% accuracy, with Bare and Snow performing best (97% recall/precision, F1=0.97–0.98). Vegetation shows 100% recall but 93% precision due to urban greenery confusion, while Built-up struggles (88% recall, 93% precision, F1=0.90) with green-roof

misclassification. Water (89% recall/precision, F1=0.89) faces reflective-surface ambiguity. Key challenges include spectral overlaps (Built-up/Vegetation, Bare/Water**)**. Improvements suggested: GLCM textures, NDBI (urban), and NDWI (water**)**. Though effective for Himalayan monitoring, the model requires refinement for urban and water-body dynamics.

Table 8: Normalised Confusion Matrix Uttarkashi produced by SVM for 2019

	Classification (Predicted)						
	Actual \ Predicted	**Bare**	**Snow**	**Vegetation**	**Built-up**	**Water**	**Producer's Accuracy/Recall**
Ground Truth (Actual)	**Bare**	0.89	0.36	0	0.07	0	0.89
	Snow	0.37	0.96	0	0	0	0.96
	Vegetation	0.23	0	0.95	0.02	0	0.95
	Built-up	0.11	0	0	0.88	0	0.88
	Water	0	0	0	0.23	0.77	0.77
	Consumer's Accuracy/precision	0.83	0.96	1	0.72	1	**Overall Accuracy = 90 %**

The Uttarkashi 2019 SVM model achieves 90% accuracy shown in Table 8, with Snow (96% recall/precision) and Vegetation (95% recall, 100% precision) performing best. Bare land (89% recall, 83% precision) shows minor confusion with Snow/Built-up, while Built-up (88% recall, 72% precision) struggles with false positives. Water has the lowest recall (77%, confused with Built-up). Key challenges include Water-Built-up reflectance and Bare-Snow spectral overlap. Recommendations: NDWI (Water), NDBI (Built-up), and texture features to improve classification. The model works well but needs refinement for urban/water features in Himalayan terrain.

Table 9: Normalised Confusion Matrix Uttarkashi produced by CART for 2024

	Classification (Predicted)						
	Actual \ Predicted	**Bare**	**Snow**	**Vegetation**	**Built-up**	**Water**	**Producer's Accuracy/Recall**
Ground Truth (Actual)	**Bare**	0.91	0	0.06	0.03	0	0.91
	Snow	0	0.96	0	0	0	1
	Vegetation	0	0	0.95	0	0	1
	Built-up	0	0	0	0.96	0.04	0.96
	Water	0	0	0	0.04	0.96	0.96
	Consumer's Accuracy/precision	1	1	0.93	0.93	0.93	**Overall Accuracy = 96.1%**

The Uttarkashi 2024 CART model achieves 96.1% accuracy, shown in Table 9 with Snow (100% recall/precision) and Bare land (100% precision, 91% recall) performing strongly. Vegetation (100% recall, 93% precision) faces false positives, while Built-up (96% recall, 93% precision) shows minor confusion with Water. Water (96% recall, 93% precision) is rarely misclassified. Key challenges include spectral overlaps (Bare ↔ Vegetation/Built-up) and reflective surfaces (Built-up ↔ Water)**.** Suggested improvements: NDVI (Vegetation), NDWI (Water), and GLCM texture analysis for urban areas. Though effective, the model requires refinement for Uttarkashi's rugged terrain. The analysis shows improved overall accuracy from 2019 to 2024 across all regions, with Uttarkashi achieving the most significant gains (+6.8% for RF). Random Forest consistently delivered the highest accuracy (≥95.4% OA in 2024), outperforming SVM and CART in most cases. All regions maintained strong classification performance in 2024, with OA scores remaining above 92.5% for all models.

The analysis of land cover categorization in Chamoli Uttarkashi and Pithoragarh, shows distinct trends in classification accuracy for various types of terrain. The distinct spectral signature of snow cover allows for relatively Accurate classification (F1 scores 0.96-1.00) however, the most consistently accurate category is

vegetation, which maintains a high accuracy (F1 0.95-1.00) because to its distinct spectral characteristics. locations with varying reflectance and shadow effects still provide obstacles. The complex nature of urban characteristics in hilly terrain, where pixel intermixing and rocky topography severely impair classification precision, and spectral mixing with bare soil cause built-up regions to exhibit high variability (F1 0.72-0.94). Due to issues such seasonal variations in water reflectance, shadow effects, and spectral similarities between fallow and bare ground, water bodies and bare land show mild performance swings (F1 0.77-0.97 and 0.83-0.97, respectively). The most reliable classifier is Random Forest, which routinely outperforms SVM and CART, especially for troublesome classifications like built-up regions where its ensemble method better manages spectral ambiguity. Although there have been noticeable increases in accuracy during the 2019–2024 era (such as Uttarkashi RF +6.8%), ongoing difficulties with built-up classification (particularly in Chamoli) and water body identification (in Pithoragarh) point to the need for methodological improvements. The main drawbacks are spectral misunderstanding between water and built-up surfaces and terrain-induced shadows that impact populated regions. In order to overcome these categorization difficulties in mountainous areas, future research should concentrate on combining terrain adjustment algorithms, higher-resolution data, and sophisticated spectral indices, especially for the most troublesome land cover classes.

Table 10: F1-Score Comparison (2019 vs 2024)

Region	**Year**	**Best Classifier**	**Bare**	**Snow**	**Vegetation**	**Built-up**	**Water**	**Key Improvement**
Uttarkashi	2019	RF	0.86	0.96	0.98	0.79	0.87	Baseline
	2024	RF	↑0.95	↑1.00	0.97	↑0.94	↑0.96	+15% Built-up
Chamoli	2019	SVM	0.94	0.96	1.00	0.90	0.96	Peak Vegetation
	2024	RF	↑0.95	↑1.00	0.98	↓0.82	0.92	+4% Bare
Pithoragarh	2019	SVM	0.91	1.00	0.97	1.00	0.97	Peak Snow
	2024	CART	↑0.97	0.98	0.97	↓0.90	↓0.89	+6% Bare

Across the Himalayan terrains, the Table 10 shows clear trends in classifier performance. Snow's distinct NIR reflectance qualities allow for near-perfect accuracy (1.00 F1 in Uttarkashi/Chamoli 2024) in classification; nonetheless, RF exhibits marginally better performance than SVM when handling shadow-affected pixels. SVM performs especially well in Chamoli's deep woods (1.00 F1 2019), and vegetation benefits from excellent NDVI separation, maintaining exceptional dependability (0.97-1.00 F1) across all regions and years.

The most variable areas are built-up (0.79-1.00 F1), where RF's ensemble technique in Uttarkashi 2024 improved accuracy by 15% compared to 2019. This was due to improved handling of spectral mixing with bare soil. However, Chamoli's 8% decline (0.90→0.82) indicates that hilly urban morphology continues to provide difficulties, since SVM's kernel techniques outperformed CART's decision boundaries.

While CART in Pithoragarh 2024 struggled with the reflectance variability of glacial-fed water (-8% accuracy), RF's multi-temporal learning in Uttarkashi improved water detection by 9%. Water bodies exhibit modest fluctuations (0.87-0.97 F1). Although Chamoli's stable but sub-perfect scores show that there are still issues with fallow-land discrimination, bare land classification increased steadily (most notably by +9% in Uttarkashi RF).

The comparison between 2019 and 2024 shows how RF is superior, with its ensemble method and comprehensive feature selection providing 6–15% accuracy gains for difficult classes.

Table 11: Overall, Area calculated by best Performance Classifiers (Area in km^2)

Region	Year	Model	Bare	Snow	Vegetation	Built-up	Water	Classified Area	Total Area	Cloud Cover
Chamoli	2019	RF	1,774.54	2,205.64	2,358.23	592.78	49.57	6,980.75	7,814	833.25
	2024	RF	1,833.06	2,388.48	2,357.82	777.14	450.34	7,806.83	7,814	7.17
Pithoragarh	2019	SVM	1,616.92	2,098.53	1,910.71	825.37	101.62	6,553.13	7,226	672.87
	2024	RF	2,334.87	1,573.41	2,349.41	313.02	647.73	7,218.45	7,226	7.56
Uttarkashi	2019	SVM	3,218.46	1,803.58	1,836.01	229.17	13.62	7,100.83	7,989	888.17
	2024	CART	2,634.54	1,998.00	2,751.93	536.88	61.18	7,982.53	7,989	6.47

The land cover classification results (in km2) for the three Himalayan areas (Chamoli, Pithoragarh, and Uttarkashi) for 2019 and 2024 are compared in Table 11 using the top-performing machine learning models (RF, SVM, and CART). Compared to Pithoragarh, which witnessed a 537% increase in water but a 25% loss in snow, Chamoli observed an 808% expansion of its water body (from 49.57 to 450.34 km2) and an 8% rise in snow cover. In Uttarkashi, the amount of vegetation recovered significantly, increasing by 50% to 2,751.93 km². Regional differences were evident in built-up areas, which decreased 62% in Pithoragarh and increased 31% in Chamoli. Significant technical advancements may be seen in the 2024 results, when 99.9% of all regions are identified, and cloud cover has decreased from 600–900 km² to less than 10 km². The most popular classifier in 2024 was Random Forest (RF), although CART did remarkably well for the vegetation of Uttarkashi. While some anomalies, such as the snow melting in Pithoragarh, need additional validation through spectral analysis and ground truthing, these discoveries also point to both real ecological changes (water expansion, vegetation regeneration) and sophisticated detection skills.

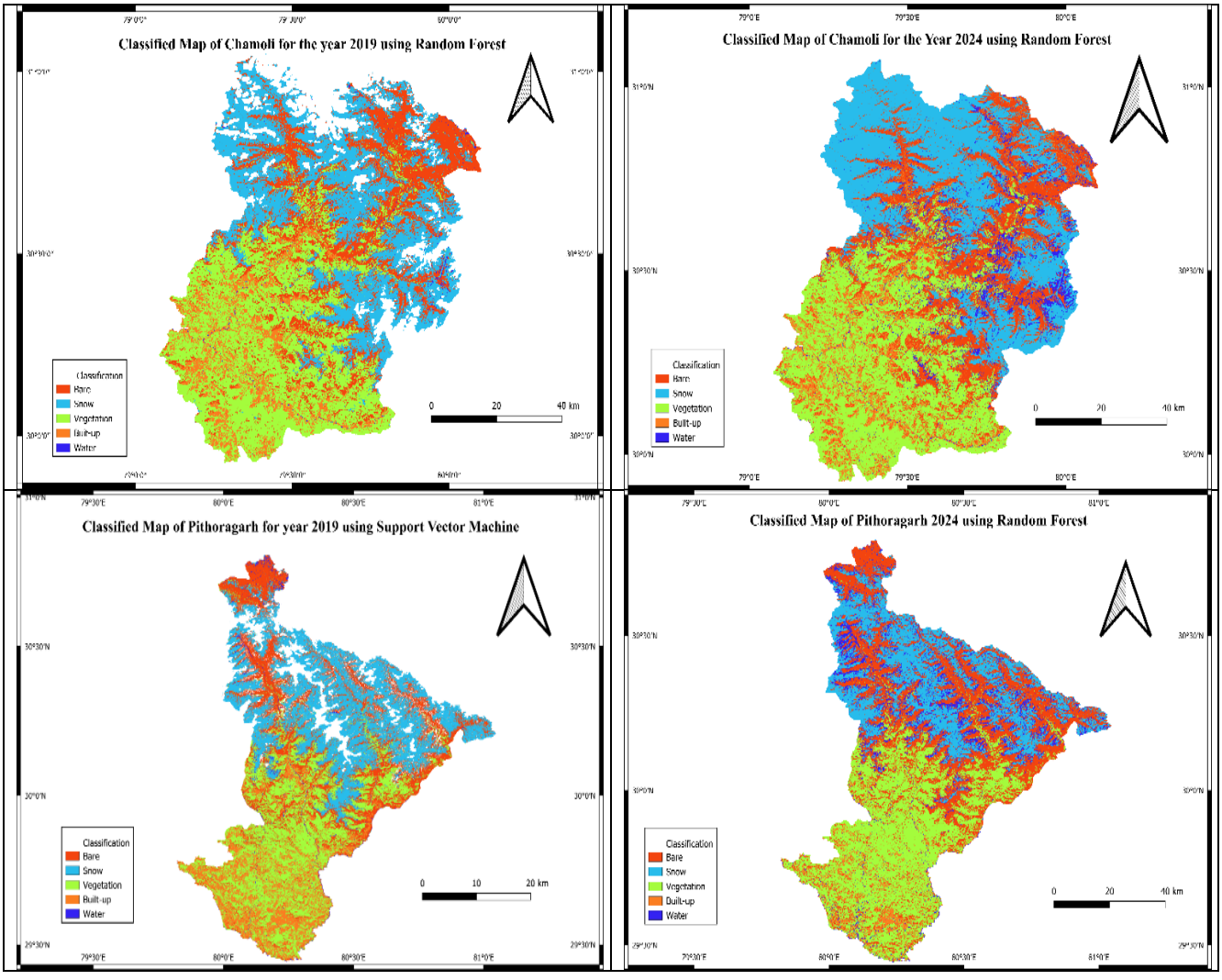

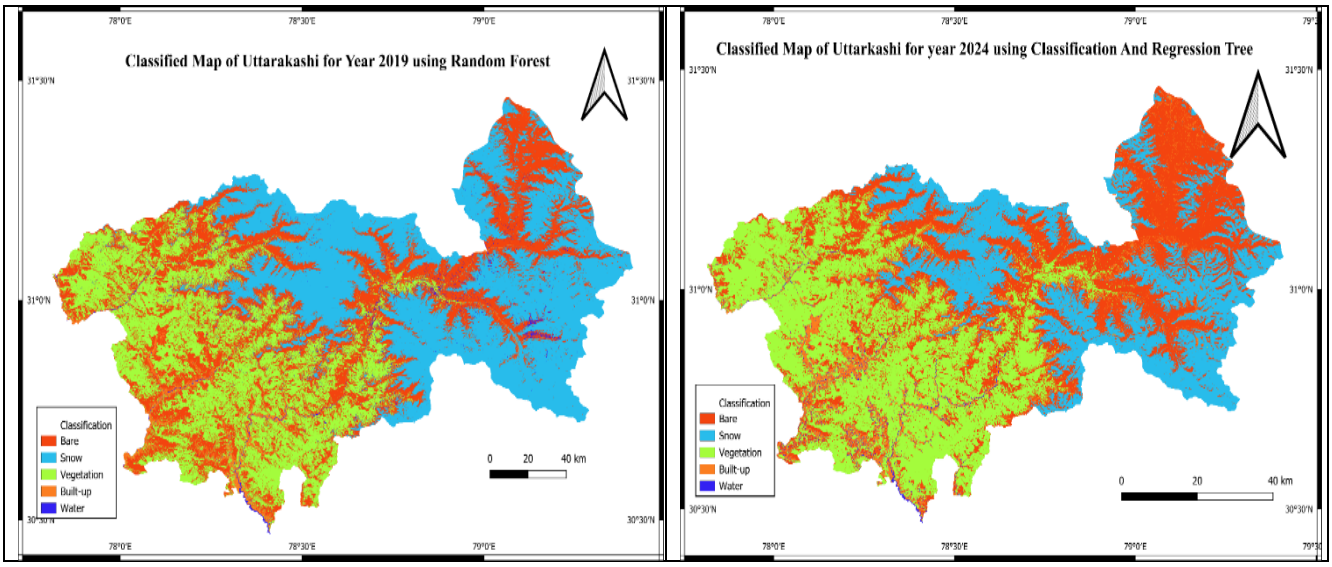

Figure 4: The classified and LULC maps and Snow cover map of Chamoli, Pithoragarh, Uttarkashi for 2019 and 2024 was created using an algorithm that achieved the highest overall accuracy.

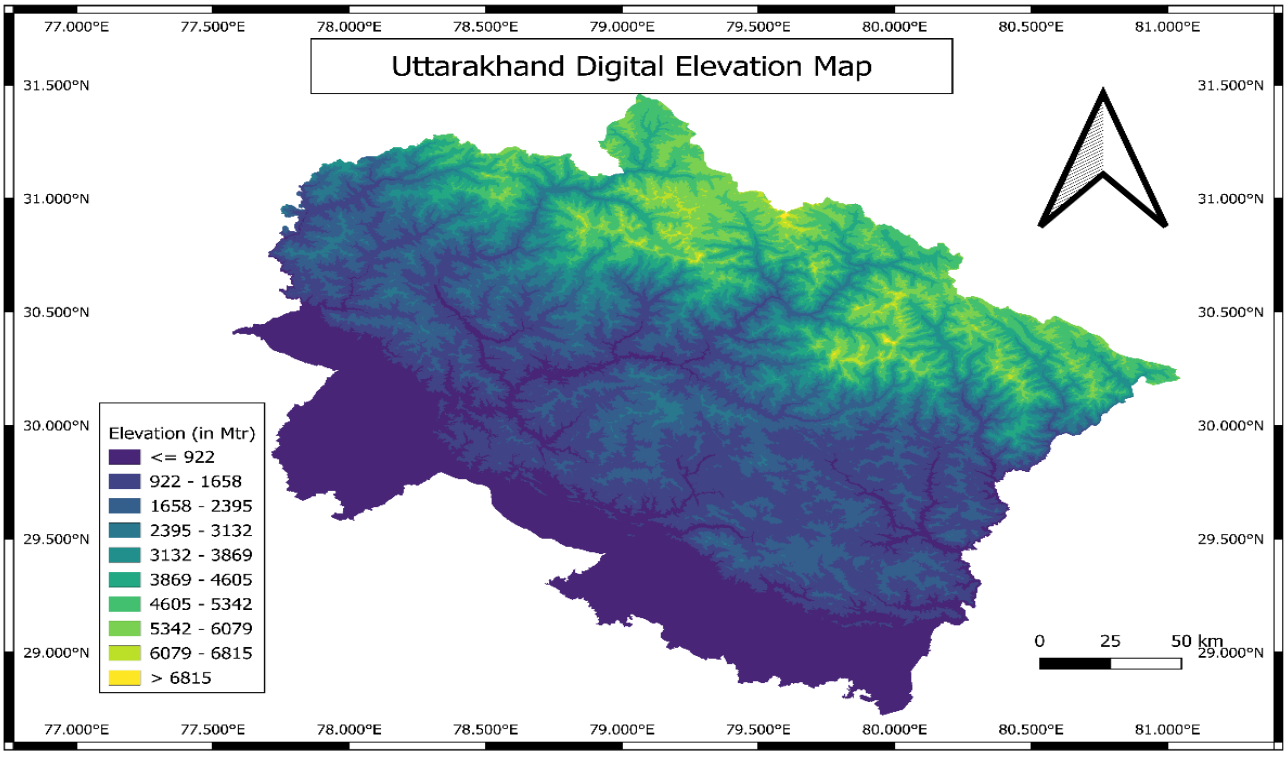

Figure 5: Digital Elevation Map of Uttarakhand

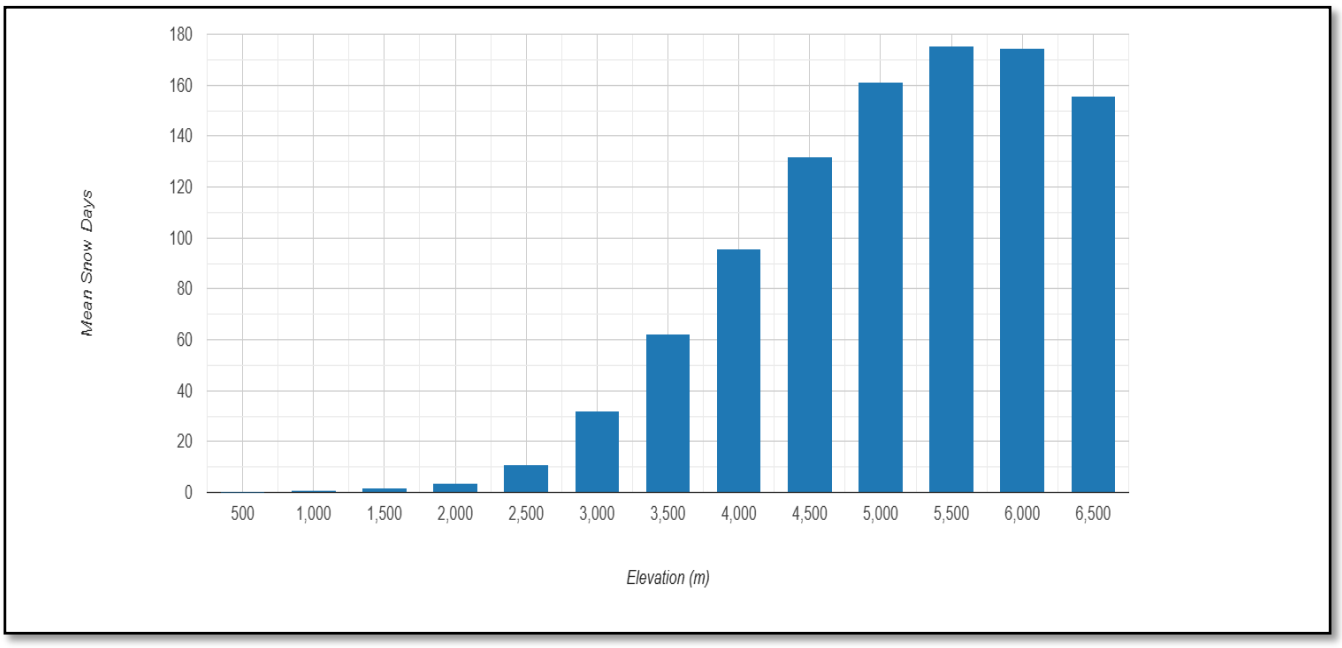

Figure 6 Mean Snow Duration (in days) Vs Elevation (in meters) for periods of year 2000-2023

Conclusion

This Research work was intended to accomplish primary objectives are as follows (i) Land Use Land Cover (LULC) Mapping. (ii) Detection of Snow cover in the Himalayan region districts of Uttarkashi, Chamoli, and Pithoragarh, Uttarakhand, India, using the annual composite median of Sentinel-2 imagery. (iii) To compare the performance of various machine learning models, that is Random Forest (RF), Support Vector Machine (SVM), and Classification and Regression Tree (CART) for 5 classes. (iv) To calculate the area of 5 classes for the years 2019 and 2024. (v) To build classified maps using the algorithm that results in the best overall accuracy shown in Figure 3. The study is located the area of Studying these LULC classes was made possible by the study area's location in a region with a variety of terrains and scenery. To encourage sustainable land use practices that benefit human communities and the environment, policymakers and planners can make better decisions by being aware of the distinctive features of each LULC. The following are the main points of the study: (i) The results of the implementation demonstrated that the RF classifier outperformed district Chamoli for the years 2019 and 2024, respectively, in terms of overall accuracy 95.7% and 96.2% and kappa value 95.7% and 96.2%., (ii) The results of the implementation demonstrated that the SVM classifier outperformed the district in 2019 with an overall accuracy of 97.3% and a kappa value of 96.6%, while RF classifier outperformed the district Pithoragarh in 2024 with an overall accuracy of 95.8% and a kappa value of 94.5%., (iii) The results of the implementation demonstrated that the RF classifier outperformed the district in 2019 with an overall accuracy of 95.5% and a kappa value of 94.4%, while RF classifier outperformed the district Pithoragarh in 2024 with an overall accuracy of 96.1% and a kappa value of 95.1%., (iv) The results indicated that most land cover classes achieved over 85% accuracy across all three classifiers (RF, SVM, and CART). The snow class showed particularly high classification accuracy (> 97%), whereas the water class had the lowest accuracy (> 88%)., (v) All classifiers in the examination of snow categorization across the Himalayan areas shown good accuracy (96–100%), with RF consistently improving, especially in Chamoli (2024). In Uttarkashi (2024) and Pithoragarh (2019), SVM and CART both received Ideal performance nonetheless, because of spectral similarities, all models consistently misidentified snow with water or sand. The most dependable performance across time and areas was shown by RF, while SVM

and CART showed regional fluctuation. These results demonstrate the robustness of the classifiers detection capabilities as well as the continuous difficulty of differentiating spectrally identical feature types in remote sensing., (vi) The study's findings showed that the study area's largest LULC class is vegetation and snow cover. Built-up and Water, on the other hand, is the smallest LULC class geographically. According to the findings, the estimated snow cover area is 2205.64 km2 by RF for 2019 and 2388.48 km2 by RF for 2024; additionally, the SVM estimates 2098.53 km2 for 2019 and 1573.41 km2 for 2024; additionally, the RF estimates 2924.72 km2 for 2019 and the CART estimates 1998 km2 for 2024., (vii) All three classifiers worked well overall and generated useful classification outcomes. Excellent LULC maps were created by every ML classifier shown in Figure 4. The study's findings showed that using a variety of satellite data, including the Harmonized Sentinel-2 MSI, VIIRS Stray Light Corrected Nighttime Day/Night Band, Digital Elevation Model (ALOS DSM: Global 30m v3.2), and WWF HydroSHEDS, is a practical way to map snow cover and LULC classes.

The study's future goals include employing remotely sensed datasets for time series analysis(Verma, Mehta and Goswami, 2022) and enhanced LULC categorization. In Future, SAR data and Landsat, combined with deep learning algorithms, can enhance LULC classification for understanding snow cover dynamics and climate change response in global mountain ecosystems.

Figure 5 shows the digital elevation Map of Uttarakhand and Figure 6 shows Uttarakhand's average annual snow cover duration in days from 2000 to 2023 in relation to elevation. MODIS MOD10A1(Hall, 2015) daily snow cover data was used to calculate the length of snow (in days/year). There is a noticeable upward trend, with longer and almost constant snow cover at higher elevations (>4000 m).

Acknowledgement The study acknowledges the European Space Agency, NASA/USGS, JAXA, Google Earth Engine (GEE), HydroSHEDS and WWF Hydrological datasets, developers of machine learning libraries, and Landsat, VIIRS, ALOS Global DSM, and hydrological datasets

Appendix

1. https://code.earthengine.google.com/c5fd11f17c405e68412de213ffe649b0
2. https://code.earthengine.google.com/546d5598d706ce989ce52d1a62a74672
3. https://code.earthengine.google.com/13719e596d43d208379ee757fd30b9fb

References

Abdi, A.M. (2020) 'Land cover and land use classification performance of machine learning algorithms in a boreal landscape using Sentinel-2 data', *GIScience and Remote Sensing*, 57(1). Available at: https://doi.org/10.1080/15481603.2019.1650447.

Asif, M., Li-Qun, Z., Zeng, Q., Atiq, M., Ahmad, K., Tariq, A., Al-Ansari, N., Blom, J., Fenske, L., Alodaini, H.A. and Hatamleh, A.A. (2023) 'Comprehensive genomic analysis of Bacillus paralicheniformis strain BP9, pan-genomic and genetic basis of biocontrol mechanism', *Computational and Structural Biotechnology Journal*, 21. Available at: https://doi.org/10.1016/j.csbj.2023.09.043.

Avtar, R., Tripathi, S., Aggarwal, A.K. and Kumar, P. (2019) 'Population-urbanization-energy nexus: A review', *Resources*. Available at: https://doi.org/10.3390/resources8030136.

Bhatt, G.D., Sinha, K., Deka, P.K. and Kumar, A. (2014) 'Flood Hazard and Risk Assessment in Chamoli District, Uttarakhand Using Satellite Remote Sensing and GIS Techniques', *International Journal of Innovative Research in Science, Engineering and Technology*, 03(08). Available at: https://doi.org/10.15680/ijirset.2014.0308039.

Billah, M., Islam, A.K.M.S., Mamoon, W. Bin and Rahman, M.R. (2023) 'Random forest classifications for landuse mapping to assess rapid flood damage using Sentinel-1 and Sentinel-2 data', *Remote Sensing Applications: Society and Environment*, 30. Available at: https://doi.org/10.1016/j.rsase.2023.100947.

Boonpook, W., Tan, Y., Nardkulpat, A., Torsri, K., Torteeka, P., Kamsing, P., Sawangwit, U., Pena, J. and Jainaen, M. (2023) 'Deep Learning Semantic Segmentation for Land Use and Land Cover Types Using Landsat 8 Imagery', *ISPRS International Journal of Geo-Information*, 12(1). Available at: https://doi.org/10.3390/ijgi12010014.

Breiman, L. (2001) 'Random Forests', *Machine Learning*, 45(1), pp. 5–32. Available at: https://doi.org/10.1023/A:1010933404324.

Breiman, L., Friedman, J.H., Olshen, R.A. and Stone, C.J. (2017) *Classification And Regression Trees*. Routledge. Available at: https://doi.org/10.1201/9781315139470.

Chachondhia, P., Shakya, A. and Kumar, G. (2021) 'Performance evaluation of machine learning algorithms using optical and microwave data for LULC classification', *Remote Sensing Applications: Society and Environment*, 23. Available at: https://doi.org/10.1016/j.rsase.2021.100599.

Choubin, B., Rahmati, O., Soleimani, F., Alilou, H., Moradi, E. and Alamdari, N. (2019) 'Regional Groundwater Potential Analysis Using Classification and Regression Trees', in *Spatial Modeling in GIS and R for Earth and Environmental Sciences*. Available at: https://doi.org/10.1016/b978-0-12-815226-3.00022-3.

Claverie, M., Ju, J., Masek, J.G., Dungan, J.L., Vermote, E.F., Roger, J.C., Skakun, S. V. and Justice, C. (2018) 'The Harmonized Landsat and Sentinel-2 surface reflectance data set', *Remote Sensing of Environment*, 219, pp. 145–161. Available at: https://doi.org/10.1016/J.RSE.2018.09.002.

Cortes, C. and Vapnik, V. (1995) 'Support-vector networks', *Machine Learning*, 20(3), pp. 273–297. Available at: https://doi.org/10.1007/BF00994018.

Defries, R.S. and Townshend, J.R. (1994) 'ndvi-derived land cover classifications at a global scale', *International Journal of Remote Sensing*, 15(17). Available at: https://doi.org/10.1080/01431169408954345.

Dou, P., Shen, H., Li, Z. and Guan, X. (2021) 'Time series remote sensing image classification framework using combination of deep learning and multiple classifiers system', *International Journal of Applied Earth Observation and Geoinformation*, 103. Available at: https://doi.org/10.1016/j.jag.2021.102477.

Duda, R.O. and Hart, P.E. (1974) 'Pattern classification and scene analysis', in *A Wiley-Interscience publication*. Available at: https://api.semanticscholar.org/CorpusID:12946615.

Goswami, S. and Ashok, A. (2024) 'Time Series Analysis of Precipitation for Uttarakhand Region', *Indian Journal of Natural Sciences*, 14(82), pp. 68315–68321.

Goswami Shikha; Ashok Alaknanda (2024) 'BURN SEVERITY ASSESSMENT IN UTTARKASHI DISTRICT, UTTARAKHAND USING SATELLITE IMAGERY AND REMOTE SENSING TECHNIQUES', *Jilin Daxue Xuebao (Gongxueban)/Journal of Jilin University (Engineering and Technology Edition)*, 43(10–2024), pp. 62–82.

Hall, D.K. and R.G.A. (2015) 'MODIS/Terra snow cover daily L3 global 500m SIN grid', *no title* [Preprint].

Kadavi, P.R. and Lee, C.-W. (2018) 'Land cover classification analysis of volcanic island in Aleutian Arc using an artificial neural network (ANN) and a support vector machine (SVM) from Landsat imagery', *Geosciences Journal*, 22(4), pp. 653–665. Available at: https://doi.org/10.1007/s12303-018-0023-2.

KHANDURİ, S. (2021) 'Flash Flood struck Dhauliganga valley on February 7, 2021: A Case study of Chamoli district of Uttarakhand Himalaya in India', *Academic Platform Journal of Natural Hazards and Disaster Management*, 2(1). Available at: https://doi.org/10.52114/apjhad.903387.

Li, Y., Brando, P.M., Morton, D.C., Lawrence, D.M., Yang, H. and Randerson, J.T. (2022) 'Deforestation-induced climate change reduces carbon storage in remaining tropical forests', *Nature Communications*, 13(1). Available at: https://doi.org/10.1038/s41467-022-29601-0.

Lu, D. and Weng, Q. (2007) 'A survey of image classification methods and techniques for improving classification performance', *International Journal of Remote Sensing*, 28(5), pp. 823–870. Available at: https://doi.org/10.1080/01431160600746456.

Mills, S., Weiss, S. and Liang, C. (2013) 'VIIRS day/night band (DNB) stray light characterization and correction', in J.J. Butler, X. (Jack) Xiong, and X. Gu (eds) *Earth Observing Systems XVIII*. SPIE, p. 88661P. Available at: https://doi.org/10.1117/12.2023107.

Nijhawan, R., Das, J. and Balasubramanian, R. (2018) 'A Hybrid CNN + Random Forest Approach to Delineate Debris Covered Glaciers Using Deep Features', *Journal of the Indian Society of Remote Sensing*, 46(6), pp. 981–989. Available at: https://doi.org/10.1007/s12524-018-0750-x.

Nijhawan, R., Das, J. and Raman, B. (2019) 'A hybrid of deep learning and hand-crafted features based approach for snow cover mapping', *International Journal of Remote Sensing*, 40(2). Available at: https://doi.org/10.1080/01431161.2018.1519277.

Noi, P.T. and Kappas, M. (2017) 'Comparison of Random Forest, k-Nearest Neighbor, and Support Vector Machine Classifiers for Land Cover Classification Using Sentinel-2 Imagery', *Sensors (Basel, Switzerland)*, 18(1). Available at: https://doi.org/10.3390/s18010018.

Oliveira, S., Oehler, F., San-Miguel-Ayanz, J., Camia, A. and Pereira, J.M.C. (2012) 'Modeling spatial patterns of fire occurrence in Mediterranean Europe using Multiple Regression and Random Forest', *Forest Ecology and Management*, 275. Available at: https://doi.org/10.1016/j.foreco.2012.03.003.

Pekel, J.-F., Cottam, A., Gorelick, N. and Belward, A.S. (2016) 'High-resolution mapping of global surface water and its long-term changes', *Nature*, 540(7633), pp. 418–422. Available at: https://doi.org/10.1038/nature20584.

Pushpalatha, V., Mahendra, H.N., Prasad, A.M., Sharmila, N., Kumar, D.M., Basavaraju, N.M., Pavithra, G.S. and Mallikarjunaswamy, S. (2024) 'An Assessment of Land Use Land Cover Using Machine Learning Technique', *Nature Environment and Pollution Technology*, 23(4), pp. 2211–2219. Available at: https://doi.org/10.46488/NEPT.2024.v23i04.025.

Qu, Y. and Long, H. (2018) 'The economic and environmental effects of land use transitions under rapid urbanization and the implications for land use management', *Habitat International*, 82. Available at: https://doi.org/10.1016/j.habitatint.2018.10.009.

Rawat, S., Saini, R., Hatture, S.K. and Shukla, P.K. (2022) 'Analysis of Post-flood Impacts on Sentinel-2 Data Using Non-parametric Machine Learning Classifiers: A Case Study from Bihar Floods, Saharsa, India', in *Smart Innovation, Systems and Technologies*. Available at: https://doi.org/10.1007/978-981-19-2719-5_14.

S, K. (2018) 'Landslide Distribution and Damages during 2013 Deluge: A Case Study of Chamoli District, Uttarakhand', *Journal of Geography & Natural Disasters*, 08(02). Available at: https://doi.org/10.4172/2167-0587.1000226.

Saini, R. and Ghosh, S.K. (2018a) 'CROP CLASSIFICATION ON SINGLE DATE SENTINEL-2 IMAGERY USING RANDOM FOREST AND SUPPOR VECTOR MACHINE', *The International Archives of the Photogrammetry, Remote Sensing and Spatial Information Sciences*, XLII–5, pp. 683–688. Available at: https://doi.org/10.5194/isprs-archives-XLII-5-683-2018.

Saini, R. and Ghosh, S.K. (2018b) 'Exploring capabilities of Sentinel-2 for vegetation mapping using random forest', in *International Archives of the Photogrammetry, Remote Sensing and Spatial Information Sciences - ISPRS Archives*. Available at: https://doi.org/10.5194/isprs-archives-XLII-3-1499-2018.

Saini, R. and Rawat, S. (2023) 'Land Use Land Cover Classification in Remote Sensing Using Machine Learning Techniques', in *1st IEEE International Conference on Innovations in High Speed Communication and Signal Processing, IHCSP 2023*. Available at: https://doi.org/10.1109/IHCSP56702.2023.10127126.

Saini, R. and Singh, S. (2024) 'Land use land cover mapping and snow cover detection in Himalayan region using machine learning and multispectral Sentinel-2 satellite imagery', *International Journal of Information Technology*, 16(2), pp. 675–686. Available at: https://doi.org/10.1007/s41870-023-01673-1.

Shen, R., Huang, A., Li, B. and Guo, J. (2019) 'Construction of a drought monitoring model using deep learning based on multi-source remote sensing data', *International Journal of Applied Earth Observation and Geoinformation*, 79. Available at: https://doi.org/10.1016/j.jag.2019.03.006.

Siddique, T., Haris, P.M. and Pradhan, S.P. (2022) 'Unraveling the geological and meteorological interplay during the 2021 Chamoli disaster, India', *Natural Hazards Research*, 2(2). Available at: https://doi.org/10.1016/j.nhres.2022.04.003.

Sridhar, V., Jin, X. and Jaksa, W.T.A. (2013) 'Explaining the hydroclimatic variability and change in the Salmon River basin', *Climate Dynamics*, 40(7–8). Available at: https://doi.org/10.1007/s00382-012-1467-0.

Sridhar, V., Kang, H. and Ali, S.A. (2019) 'Human-induced alterations to land use and climate and their responses for hydrology and water management in the Mekong River Basin', *Water (Switzerland)*, 11(6). Available at: https://doi.org/10.3390/w11061307.

Stehfest, E., van Zeist, W.-J., Valin, H., Havlik, P., Popp, A., Kyle, P., Tabeau, A., Mason-D'Croz, D., Hasegawa, T., Bodirsky, B.L., Calvin, K., Doelman, J.C., Fujimori, S., Humpenöder, F., Lotze-Campen, H., van Meijl, H. and Wiebe, K. (2019) 'Key determinants of global land-use projections', *Nature Communications*, 10(1), p. 2166. Available at: https://doi.org/10.1038/s41467-019-09945-w.

Tadono, T., Ishida, H., Oda, F., Naito, S., Minakawa, K. and Iwamoto, H. (2014) 'Precise Global DEM Generation by ALOS PRISM', *ISPRS Annals of the Photogrammetry, Remote Sensing and Spatial Information Sciences*, II–4, pp. 71–76. Available at: https://doi.org/10.5194/isprsannals-II-4-71-2014.

Tariq, A., Shu, H., Siddiqui, S., Imran, M. and Farhan, M. (2021) 'Monitoring land use and land cover changes using geospatial techniques, a case study of Fateh Jang, Attock, Pakistan', *Geography, Environment, Sustainability*, 14(1). Available at: https://doi.org/10.24057/2071-9388-2020-117.

Tariq, A., Yan, J., Gagnon, A.S., Khan, M.R. and Mumtaz, F. (2023) 'Mapping of cropland, cropping patterns and crop types by combining optical remote sensing images with decision tree classifier and random forest', *Geo-Spatial Information Science*, 26(3). Available at: https://doi.org/10.1080/10095020.2022.2100287.

Tsai, Y.L.S., Dietz, A., Oppelt, N. and Kuenzer, C. (2019) 'Remote sensing of snow cover using spaceborne SAR: A review', *Remote Sensing*. Available at: https://doi.org/10.3390/rs11121456.

Verma, G., Mehta, A. and Goswami, S. (2022) 'Trend and Time Series Analysis of Vegetation Dynamics Using Satellite Data: A Case Study of Uttarakhand, India', *Current Journal of Applied Science and Technology*, 41(33), pp. 14–26. Available at: https://doi.org/https://doi.org/10.9734/cjast/2022/v41i333947.

Zheng, X., Sarwar, A., Islam, F., Majid, A., Tariq, A., Ali, M., Gulzar, S., Khan, M.I., Ali, M.A.S., Israr, M., Jamil, A., Aslam, M. and Soufan, W. (2023) 'Rainwater harvesting for agriculture development using multi-influence factor and fuzzy overlay techniques', *Environmental Research*, 238. Available at: https://doi.org/10.1016/j.envres.2023.117189.